J. Fluid Mech. (1998), *vol.* 372, *pp.* 213–230. Printed in the United Kingdom

© 1998 Cambridge University Press

Quasi-steady vortical structures in vertically vibrating soap films

By JOSÉ M. VEGA[1], F. J. HIGUERA[1] AND P. D. WEIDMAN[2]

[1]E. T. S. Ingenieros Aeronáuticos, Plaza Cardenal Cisneros 3, 28040 Madrid, Spain
[2]Department of Mechanical Engineering, University of Colorado, Boulder, CO 80309, USA

(Received 7 January 1998 and in revised form 13 May 1998)

An analysis of the quasi-steady streaming of the liquid in a vertically vibrated horizontal soap film is reported. The air around the soap film is seen to play a variety of roles: it transmits normal and tangential oscillatory stresses to the film, damps out Marangoni waves, and forces non-oscillatory deflection of the film and tangential motion of the liquid. Non-oscillatory volume forcing originating inside the liquid is also analysed. This forcing dominates the quasi-steady streaming when the excitation frequency is close to the eigenfrequency of a Marangoni mode of the soap film, while both volume forcing in the liquid and surface forcing of the gas on the liquid are important when no Marangoni mode resonates. Different manners by which the combined forcings can induce quasi-steady streaming motion are discussed and some numerical simulations of the quasi-steady liquid flow are presented.

1. Introduction

Liquid flow in stationary soap films is essentially two-dimensional owing to the extremely small thickness of these films. This led Gharib & Derango (1989) and others to propose that soap film systems may provide a means for experimentally simulating two-dimensional hydrodynamics. Analysis, however, has shown that the fluid motion in soap films is much more complex than standard hydrodynamics, due to a number of peculiar phenomena that include surfactant transport through evaporation, finite disturbance propagation speeds connected with the not-fully-understood properties of surfactants, and the possibility of irreversible formation of regions of black film where the two micelle interfaces come into contact. Studies of the physical properties and the statics of soap films date back to the pioneering works of Plateau (1873) and Gibbs (1931), and soap films have received recurrent attention in the literature ever since, due to their value as a simulating tool and to the richness of their own dynamics. Vortical motion in thin films, in particular, has been very much studied, beginning with the work of Couder (1981). Many different types of forcing and flow configurations have been considered, including laminar and turbulent wakes behind obstacles or arrays of obstacles in relative motion to the film (Couder 1984; Couder & Basdevant 1986; Rutgers, Wu & Bhagatula 1996; and Martin, Wu & Goldburg 1998), motions induced in the liquid by the impingement or shear of a surrounding air stream (Rabaud & Couder 1983; Chomaz *et al.* 1988), and flows due to the combined action of gravity and surface tension (Couder, Chomaz & Rabaud 1989). Reviews of the known physics of soap films and descriptions of the impressive variety of flows that they can sustain are given by Rusanov & Krotov (1979) and Couder *et al.* (1989).

https://doi.org/10.1017/S0022112098002225 Published online by Cambridge University Press

Vibrating soap films were observed by Taylor (1878), who reported coloured fringe patterns and steady vortical motions in films excited by sound waves, and by Bergmann (1956), who obtained very clean photographs of a film excited by a loudspeaker and subject to rotation to make its thickness uniform. More quantitative experiments were carried out by Airiau (1986) and Afenchenko *et al.* (1998) using different excitation devices. In both of these experiments the frame holding the film was rigidly and symmetrically attached to the lateral walls of a cavity, in order to reduce evaporation and contamination of the film, and shield the film from external disturbances. In the experiments of Airiau the excitation was provided by a loudspeaker fitted to the bottom of the cavity, which was otherwise open. It was observed that the mode of the film excited by the loudspeaker depends on the frequency, and that in narrow transition ranges where two modes coexist with comparable amplitude, their phases are different and shift with changing frequency. Liquid accumulates in the crests of the modes a short time after starting the vibration, and this leads to the accumulation of interference fringes when the film is illuminated with monochromatic light. Recirculation of the liquid begins shortly afterwards in the regions of small thickness surrounding the crests, where patches of black film are eventually formed. The migration of liquid toward the crests was explained as a secondary motion due to surface tension forces.

The cavity containing the soap film in the experiments of Afenchenko *et al.* (1998) was closed and mounted on an electro-mechanical vibrator. While this setup minimizes evaporation and unwanted disturbances, it leads to some uncertainty as to the excitation mechanism. These authors concluded that the strength of vortices in a given vortex pattern increases with increasing external forcing and with decreasing film thickness. In their visualizations, initially thick films produced incoherent light interference which provided shadowgraph images of the planform structure of transverse oscillations, while organized interference patterns, consisting of coloured fringes, appeared when the film thinned by evaporation. Vortex motion was observed in regions of low fringe density, which is where the film is thinnest, and these regions coexist with 'bladders' of much larger thickness. A theoretical description of the vortical motion was proposed based on the assumption of viscous diffusion from the perimeter of the film, where standard results on steady streaming generated by relative oscillatory motion between a fluid and its solid boundary (see, for example, Schlichting 1951 and the recent review by Riley 1997) were supposed to be applicable to the Stokes layer associated with Marangoni waves in the liquid. Afenchenko *et al.* (1998) recognized, however, that this diffusive model could not explain the spontaneous appearance, at the film's interior, of vortices pinned to specific points on the planform pattern of flexural mode vibrations.

In this paper a systematic qualitative analysis is presented of the generation of steady or quasi-steady vortical motions in vertically vibrated horizontal films. As we shall see, the air surrounding the film plays an important role in typical experimental conditions (a fact already pointed out by Airiau 1986) and this will make the analysis somewhat involved. For the sake of clarity, we restrict ourselves to the case when the oscillating flows in the air and the liquid obey linear problems and are decoupled from the quasi-steady motions. Some of the complex behaviours observed by Afenchenko *et al.* (1998) are thereby excluded from the analysis.

The problem is formulated in § 2. Equations governing the leading-order oscillatory flow both in the air and in the liquid, and the leading-order quasi-steady non-oscillatory flow in the liquid are set forth in § 3. Numerical solutions exhibiting some

https://doi.org/10.1017/S0022112098002225 Published online by Cambridge University Press

of the vibration-induced vortex motions in the film are presented in § 4 and concluding remarks are given in § 5.

2. Problem formulation

Consider a thin soap film of thickness e stretched on a plane, horizontal frame. The film is forced to oscillate vertically with frequency ω, either by a vibration of the frame, as in the experiment of Afenchenko *et al.* (1998), or of the surrounding air, whose motion can be due to the vibration of a nearby solid, as in the experiment of Airiau (1986), or to an acoustic wave impinging on the film, as in the early observations of Taylor (1878). The oscillations of both the air and the liquid are assumed to be essentially linear and monochromatic which, according to the ensuing analysis, is justified if the amplitude of the excitation is sufficiently small and higher-order harmonics of integer multiples of ω do not resonate. Liquid evaporation and the formation of black film are not accounted for in the analysis.

The motion of the air around the film obeys the incompressible continuity and Navier–Stokes equations with no-slip conditions at the surfaces of the film and either no-slip conditions at the vibrating or stationary solid walls bounding the film and the surrounding air, or conditions of zero velocity far away from the film and the source of the oscillations if they are not fully enclosed by solid walls. An exception to this latter condition is when the oscillation of the film is forced by an acoustic wave propagating in the air, in which case the flow far from the film is that of the oncoming wave plus the waves reflected and transmitted by the film. In any event, the oscillatory motion of the air and the associated oscillatory deflection of the film can be straightforwardly calculated, at least in principle, and their effect on the liquid phase, leading to the generation of steady or quasi-steady structures inside the film, may then be analysed.

In order to formulate the problem in the liquid phase let $\boldsymbol{x} = (x, y)$ be Cartesian coordinates in the plane of the unperturbed film, $\nabla = (\partial/\partial x, \partial/\partial y)$ the corresponding horizontal gradient operator, $\boldsymbol{v} = (u, v)$ the horizontal coordinate velocities of the liquid averaged across the film, and z the distance from the centreplane of the unperturbed film. The deflection and thickness of the film, $f(\boldsymbol{x}, t)$ and $e(\boldsymbol{x}, t)$, are defined such that the interfaces lie at $z = f \pm e/2$ and will be supposed to satisfy $e \ll f \ll l$, where l is the characteristic length of the flow along the film. To an approximation sufficient for our purposes, the continuity and momentum equations describing the motion of the liquid are

$$\frac{\partial e}{\partial t} + \nabla \cdot (e\boldsymbol{v}) = 0, \tag{2.1}$$

$$e\frac{\partial \boldsymbol{v}}{\partial t} + e\boldsymbol{v} \cdot \nabla \boldsymbol{v} = \frac{2}{\rho}\nabla\sigma - e\left(\frac{\partial^2 f}{\partial t^2} + g\right)\nabla f + \frac{1}{\rho}\nabla \cdot \tau' + 2\nu\nabla(e\nabla \cdot \boldsymbol{v}) + \frac{1}{\rho}\boldsymbol{\tau}_g, \tag{2.2}$$

and

$$\rho e\left(\frac{\partial^2 f}{\partial t^2} + g + 2\boldsymbol{v} \cdot \nabla\frac{\partial f}{\partial t}\right) = 2\sigma\nabla^2 f - \Delta p_g. \tag{2.3}$$

The subscript g is attached to stresses produced on the film by the gas phase. The surface tension coefficient σ is a function of the local surface concentration of soap, which in turn depends only on the local thickness e of the film if the concentration is initially uniform; see Rusanov & Krotov (1979) and Couder *et al.* (1989). In (2.2),

https://doi.org/10.1017/S0022112098002225 Published online by Cambridge University Press

$(\partial^2 f/\partial t^2+g)\nabla f$ is the projection of the vertical acceleration of the liquid on the tangent to the film, with g the gravitational acceleration; $\tau'_{ij} = \rho(ev + v^s)(\partial v_i/\partial x_j + \partial v_j/\partial x_i)$ is the overall viscous stress tensor containing contributions from the bulk liquid and its interfaces, with respective viscosities ρv and ρv^s (see Rusanov & Krotov 1979 and Couder *et al.* 1989); $2v\nabla(e\nabla\cdot\boldsymbol{v})$ is the gradient of the pressure variation appearing in the liquid to balance the normal viscous stress associated with the straining of the film (see Jenkins & Dysthe 1997); and $\boldsymbol{\tau}_g$ is the sum of the shear stresses of the air on both sides of the film. The term $2\boldsymbol{v}\cdot\nabla\partial f/\partial t$ in (2.3) is a Coriolis-like acceleration due to the local rotation of the film, and $\Delta p_g = p_g^+ - p_g^-$ is the difference of air pressures above and below the film.

Equations (2.1) and (2.2) resemble the continuity and momentum equations of a gas of bulk viscosity $\frac{8}{3}ev$, with e and $-2\sigma(e)/\rho$ playing the roles of density and pressure, and $a = [-2(\mathrm{d}\sigma/\mathrm{d}e)/\rho]^{1/2}$ playing the role of the speed of sound. In what follows the 'relation of barotropy' $\sigma = \sigma_0 - ce/(e+k)$, where σ_0, c and k are constants, will be used. This relation is valid for dilute soap solutions, with concentrations smaller than the critical micelles concentration, and oscillation periods shorter than the bulk-surface thermodynamic relaxation time; again see Couder *et al.* (1989) and Rusanov & Krotov (1979) for details. Typical values are $k \approx 8\,\mu\mathrm{m}$ and $a \approx 1$–$10\,\mathrm{m\ s^{-1}}$.

Equations (2.1)–(2.3) can be derived by writing their fully three-dimensional counterparts in a curvilinear coordinate system attached to the film and averaging across the film or, equivalently, by establishing the mass and momentum balances for a control volume bounded by the interfaces and the cross-section along a closed curve. In either way, both the averaging process and the projection on the horizontal plane lead to further terms of order $|\nabla f|^2 + (e/l)^2 \ll 1$ relative to the ones displayed. Other small effects neglected in (2.2) are the pressure gradient tangent to the film, the difference of surface tension forces between the two interfaces, and some small terms associated with the curvature of the film. Finally, the gas viscous stresses normal to the interfaces have been left out of (2.3).

The velocity and pressure in the air and the deflection of the film will be decomposed into oscillatory and non-oscillatory parts as

$$\left.\begin{aligned}(\boldsymbol{v}_g, w_g, p_g) &= (\boldsymbol{V}_g, W_g, P_g)\,\mathrm{e}^{\mathrm{i}\omega t} + \mathrm{cc} + (\boldsymbol{v}_{gs}, w_{gs}, p_{gs}) + \mathrm{HOH},\\ f &= F\,\mathrm{e}^{\mathrm{i}\omega t} + \mathrm{cc} + f_s + \mathrm{HOH},\end{aligned}\right\} \tag{2.4}$$

where complex notation is used, with cc denoting complex conjugate, and HOH means higher-order harmonics at integer multiples of ω, which will be assumed to be small compared to the leading oscillatory term. The subscript s denotes a non-oscillatory flow component. The horizontal and vertical gas-phase velocity components are $\boldsymbol{v}_g$ and w_g, and the gas-phase pressure is p_g. $\boldsymbol{V}_g$, W_g, P_g and $\boldsymbol{v}_{gs}$, w_{gs}, p_{gs} depend on $\boldsymbol{x}$ and z, and F and f_s depend on $\boldsymbol{x}$ only. These quantities also may depend on time, in a characteristic time scale much larger than ω^{-1}, and consequently these terms are described as being quasi-steady or non-oscillatory throughout the paper. Similarly, the thickness of the film and the liquid velocity are decomposed as

$$\left.\begin{aligned}e &= E\,\mathrm{e}^{\mathrm{i}\omega t} + \mathrm{cc} + e_s + \mathrm{HOH},\\ \boldsymbol{v} &= \boldsymbol{V}\,\mathrm{e}^{\mathrm{i}\omega t} + \mathrm{cc} + \boldsymbol{v}_s + \mathrm{HOH},\end{aligned}\right\} \tag{2.5}$$

with the same notation as above. Again the quantities on the right-hand sides depend on $\boldsymbol{x}$ and are allowed to vary slowly with time.

https://doi.org/10.1017/S0022112098002225 Published online by Cambridge University Press

3. Analysis

The linear problems describing the leading oscillatory flows in the air and in the liquid, and the equations governing the quasi-steady, non-oscillatory flow in the liquid will be derived in § 3.1 and § 3.2, respectively. The range of non-oscillatory flow regimes encompassed by these latter equations will be discussed in § 3.3. We have not introduced a particular scaling at this point because of the numerous characteristic length and time scales involved in the problem, some of which span several orders of magnitude in realistic experimental conditions. This makes the analysis somewhat subtle, but inconsistencies will be avoided by carefully ensuring, at each step, that neglected terms are in fact small compared to those retained, under assumptions that will be invoked when needed. After appropriate scalings are introduced in the equations derived below, several dimensionless parameters will appear in a natural way.

3.1. *Oscillatory flow*

Consider first the leading oscillatory terms of expansions (2.4) and (2.5). These terms satisfy the linearized forms of the continuity and momentum equations in the air, the linearized forms of equations (2.1) and (2.2) in the liquid, and of equation (2.3) across the film, as well as conditions of continuity of the velocity at the film surfaces. In what follows all these equations will be linearized around the quiescent state, which is admissible if the conditions $\omega|F| + |\boldsymbol{v}_{sg}| + |w_{sg}| \ll \omega l$ and $|\boldsymbol{V}| + |\boldsymbol{v}_s| \ll \omega l$ are satisfied.

The linearized problem in the air can be simplified in the realistic case $\omega l^2 \gg \nu_g$, for which the effect of the air viscosity is confined to Stokes layers of characteristic thickness $\delta = (\nu_g/\omega)^{1/2} \ll l$ on both sides of the film and on the solid walls. If, in addition, the thickness of the film is sufficiently small (recall that $e \ll l$), then the oscillations of the film and the air outside the Stokes layers obey

$$\nabla \cdot \boldsymbol{V}_g + \frac{\partial W_g}{\partial z} = 0, \tag{3.1}$$

$$\mathrm{i}\rho_g \omega \boldsymbol{V}_g = -\nabla P_g, \tag{3.2}$$

$$\mathrm{i}\rho_g \omega W_g = -\frac{\partial P_g}{\partial z}, \tag{3.3}$$

$$z = 0 : \begin{cases} W_g^{\pm} = \mathrm{i}\omega F, & (3.4a) \\ P_g^{+} - P_g^{-} = \rho e_s \omega^2 F + 2\sigma_s \nabla^2 F, & (3.4b) \end{cases}$$

plus the inviscid conditions $(\boldsymbol{V}_g, W_g) \cdot \boldsymbol{n} = V_{wall}$ at a solid wall vibrating with velocity $V_{wall}\ \exp(\mathrm{i}\omega t) + \mathrm{cc}$ in the direction of its normal $\boldsymbol{n}$, and $(\boldsymbol{V}_g, W_g, P_g) \to 0$ as $(\boldsymbol{x}, z) \to \infty$, if the film is not enclosed by solid walls. Here the superscripts $\pm$ denote conditions above and below the film. The two terms on the right hand side of boundary condition (3.4*b*) reflect the influence of the film on the oscillations of the air through the inertia of the liquid and the surface tension of the interfaces, respectively.

Equations (3.2) or (3.3) along with (3.4*a*) yield the estimate $P_g = O(\rho_g \omega^2 |F| l)$ and, consequently, $\rho e_s \omega^2 F/P_g = O(\rho e/\rho_g l)$ and $2\sigma_s \nabla^2 F/P_g = O(\sigma/\rho_g \omega^2 l^3)$. For typical values of the magnitudes involved (namely $\rho/\rho_g \approx 10^3$, $l \sim 1$–$5\,\mathrm{cm}$, $\sigma \sim 20$–60 dyn cm^{-1} and $\omega/2\pi \sim 30$–100 Hz), the first of these ratios ranges from order one for thick films ($e > 10\,\mu\mathrm{m}$) to small values, and the second ratio is of order one. Thus *the inertia of the liquid never dominates over that of the air*, and hence the air cannot be ignored in the analysis of the oscillations.

https://doi.org/10.1017/S0022112098002225 Published online by Cambridge University Press

Once $\boldsymbol{V}_g^{\pm}$ is known from the solution of the inviscid gas-phase problem, the oscillatory flow in the Stokes layers can be determined. In terms of the distances to the interfaces, $\eta = z - (f \pm e/2)$, the horizontal oscillatory velocities of the air in the layers above and below the film are

$$\{\boldsymbol{V}_g^{\pm} + (\boldsymbol{V} - \boldsymbol{V}_g^{\pm}) \exp(\mp\sqrt{\mathrm{i}}\eta/\delta)\}\mathrm{e}^{\mathrm{i}\omega t} + \mathrm{cc}, \tag{3.5}$$

where $\boldsymbol{V}_g^{\pm} = \boldsymbol{V}_g(\boldsymbol{x}, y, 0^{\pm})$ and, as defined above, $\delta = (\nu_g/\omega)^{1/2}$.

Problem (3.1)–(3.4) with homogeneous boundary conditions at the solid walls determines the *flexural modes* of the air–film system for which the balance of the inertia of the liquid and the air with the restoring surface tension force yields the estimate $\omega^2 l^2 = O[2\sigma/(\rho e + \rho_g l)]$; see Couder *et al.* (1989) and Taylor (1959). The damping rate of a flexural mode of frequency ω due to viscous dissipation in the Stokes layers is $\gamma_{_F} = O(\omega\delta/l)$, which is also the order of the frequency window of linear resonance. Thus the characteristic amplitudes of the oscillation ($A = \max|F|$, say) and of the forcing ($A_0 = \max|V_{wall}|/\omega$) satisfy $A = O(A_0\omega/\gamma_{_F})$ if the difference between the forcing frequency and the frequency of a flexural mode is of order $\gamma_{_F}$, and $A = O(A_0)$ otherwise.

Equations (3.1)–(3.4) are invariant under the symmetry transformation $z \to -z$, $\boldsymbol{V}_g \to -\boldsymbol{V}_g$, $P_g \to -P_g$. If the boundary conditions are also invariant under this transformation (as is the case in the experiment of Afenchenko *et al.* 1998) then the solution is invariant. This means that non-degenerate flexural modes are invariant under the above transformation if the container and far-field boundaries are symmetric in z. As a consequence, the solution in the resonant case when the forcing frequency is close to an inviscid eigenfrequency is, to a first approximation, invariant under this transformation even if the forcing device is not symmetric. A similar discussion is applicable to the transformation $z \to -z$, $W_g \to -W_g$, $F \to -F$, which also leaves equations (3.1)–(3.4) invariant. Now, however, invariance of a solution under this second transformation implies that $F \equiv 0$, a condition that no flexural mode can fulfil.

We note for future reference that the solution of (3.1)–(3.4) is a wave with a spatially uniform phase unless (*a*) there is more than a single forcing device (e.g. more than one vibrating wall) with phase shifts different from 0 and π and their frequency is not close to any eigenfrequency of the system, or (*b*) the forcing frequency is close to that of a degenerate or nearly degenerate eigenmode.

The linearized forms of equations (2.1) and (2.2), determining $\boldsymbol{V}$ and E (cf. (2.5)), are

$$\mathrm{i}\omega E + \nabla\cdot(e_s\boldsymbol{V}) = 0, \tag{3.6a}$$

$$\mathrm{i}\omega e_s\boldsymbol{V} = -\nabla\left(a_s^2 E\right) + \frac{\boldsymbol{T}_g}{\rho} + \omega^2 e_s(\nabla f_s)F - g e_s\nabla F, \tag{3.6b}$$

where $a_s^2 = a^2(e_s) = -2[\mathrm{d}\sigma(e_s)/\mathrm{d}e_s]/\rho$ and $\boldsymbol{T}_g\mathrm{e}^{\mathrm{i}\omega t} + \mathrm{cc}$, with $\boldsymbol{T}_g = \sqrt{\mathrm{i}}(\rho_g\nu_g/\delta)(\boldsymbol{V}_g^{+} + \boldsymbol{V}_g^{-} - 2\boldsymbol{V})$, is the oscillatory viscous stress of the gas on both sides of the film. Viscous terms, of order $(\nu + \nu^s/e)/\omega l^2$ relative to the inertial terms, have been left out of equation (3.6*b*). A term $-gE\nabla f_s$ has been also omitted in the right-hand side of this equation because we are assuming that $g|\nabla f_s| \ll a_s^2/l$, which is usually the case in practice. For the same reason, a term $-\rho g E$ was omitted in the right-hand side

https://doi.org/10.1017/S0022112098002225 Published online by Cambridge University Press

of linearized boundary condition (3.4*b*). From equation (3.6*a*) the relative thickness variation is $E/e_s = O(|\boldsymbol{V}|/\omega l) \ll 1$. Elimination of E from the latter two equations and substitution of $\boldsymbol{T}_g$ yields

$$\mathrm{i}\omega e_s \boldsymbol{V} - \frac{1}{\mathrm{i}\omega}\nabla\left[a_s^2 \nabla\cdot(e_s\boldsymbol{V})\right] + 2\sqrt{\mathrm{i}}\frac{\rho_g}{\rho}\frac{\nu_g}{\delta}\boldsymbol{V} = \sqrt{\mathrm{i}}\frac{\rho_g}{\rho}\frac{\nu_g}{\delta}(\boldsymbol{V}_g^+ + \boldsymbol{V}_g^-) + \omega^2 e_s(\nabla f_s)F - g e_s \nabla F, \quad (3.7)$$

to be solved with appropriate conditions around the perimeter of the film, dependent on the mode of attachment of the film to its support frame.

The operator acting on $\boldsymbol{V}$ in the left-hand side of (3.7) describes the Marangoni waves in the film which owe their existence to spatial variations of surface tension with film thickness. The phase speed of these waves is a_s in the absence of damping. The third term on the left-hand side represents the damping by dissipation in the Stokes layers that the Marangoni waves generate in the air. The damping rate of waves of frequency ω is $\gamma_M = R\omega/\sqrt{2}$, where $R = (\rho_g\delta)/(\rho e_c)$ is the ratio of the mass of air in the Stokes layers to the mass of liquid in the film when e_c is the characteristic value of the film thickness. This ratio is moderately small for typical frequencies, in the range 30–100 Hz, and for all but very thin films less than 0.1 μm. If the forcing frequency differs by an amount of order γ_M from the frequency of a Marangoni mode then (3.7) gives $|\boldsymbol{V}| = O\left\{|\boldsymbol{V}_g^+ + \boldsymbol{V}_g^-| + |\nabla f_s||\boldsymbol{V}_g^\pm|/R + g|\boldsymbol{V}_g^\pm|/(\omega^2 l R)\right\}$; otherwise $|\boldsymbol{V}|$ is R times smaller. It is also worth noting that flexural and Marangoni modes may resonate simultaneously for some forcing frequencies, because the phase speeds of the two kinds of waves are of the same order and some of the resonances are not very narrow.

The three terms on the right-hand side of (3.7) reflect the excitation of Marangoni waves by flexural oscillations of the air and the film. In the order given, these terms represent the viscous tangential stress of the gas on the interfaces, the projection of the vertical oscillatory acceleration of the liquid on the time-averaged, quasi-steady film, and the projection of the gravitational acceleration on the oscillatory film, respectively. The ratios of the second and third terms to the first one, of orders $|\nabla f_s|/R$ and $g/(\omega^2 l R)$, are frequently small except for thick films and low frequencies. These two terms, however, provide the only mechanism forcing Marangoni waves in the symmetric case $\boldsymbol{V}_g^+ + \boldsymbol{V}_g^- = \boldsymbol{0}$.

3.2. *Quasi-steady streaming flow*

We turn now to the non-oscillatory terms of expansions (2.4) and (2.5), which are due to the nonlinearity of the governing equations and will be denoted by a subscript s. Consider first the gas phase, where the only nonlinear terms are the convective terms of the momentum equations. Outside the Stokes layers the leading-order oscillatory velocity is potential, and so are the convective terms when evaluated with this velocity, leading only to the non-oscillatory pressure variation $\Delta p_{gs} = -\rho_g(|\boldsymbol{V}_g|^2 + |W_g|^2)$. Then the non-oscillatory pressures in the gas just above and below the film are $p_{gs}^\pm = -\rho_g\left(|\boldsymbol{V}_g^\pm|^2 + \omega^2|F|^2\right) - \rho_g g f_s$ in the first approximation. Substituting this result into (2.3) and collecting non-oscillatory terms yields

$$2\sigma\nabla^2 f_s = -\rho_g\left(|\boldsymbol{V}_g^+|^2 - |\boldsymbol{V}_g^-|^2\right) - \rho g e_s - \rho\omega\left[\mathrm{i}\bar{F}\nabla\cdot(e_s\boldsymbol{V}) + 2\mathrm{i}e_s\boldsymbol{V}\cdot\nabla\bar{F} + \mathrm{cc}\right], \quad (3.8)$$

where, as above, $\boldsymbol{V}_g^\pm = \boldsymbol{V}_g(\boldsymbol{x}, y, 0^\pm)$, with $\boldsymbol{V}_g$ given by the solution of (3.1)–(3.4), and

https://doi.org/10.1017/S0022112098002225 Published online by Cambridge University Press

E has been eliminated using equation (3.6*a*). In (3.8) and hereafter an overbar denotes complex conjugate. The pressure variation across the Stokes layers above and below the film have been omitted since they are R times the pressure variation in the liquid across the film, as given by the last two terms on the right-hand side of (3.8), which themselves come from the last two terms on the left-hand side of (2.3). This simplification is valid if R is small, which happens for all but very thin films as noted in the discussion following (3.7). Even for such thin films, the simplification is valid because the pressure variation in the liquid across the film and the omitted term can be neglected altogether.

Consider next the quasi-steady streaming of the liquid. Non-oscillatory forcing terms appear in the momentum equation (2.2) due to the tangential stress of the gas on the interfaces, $\boldsymbol{\tau}_g$, and to the nonlinear terms of this equation involving products of quantities pertaining to the liquid film. These two types of forcing will be discussed in turn.

In order to evaluate the non-oscillatory part of $\boldsymbol{\tau}_g/\rho$ the motion of the air inside and outside the Stokes layers surrounding the film must be analysed separately. Inside these layers, where oscillatory vorticity parallel to the interfaces exists, the oscillatory vertical velocity, obtained from the continuity equation, is

$$\left\{ \mathrm{i}\omega F - \nabla(f_s \pm e_s/2)\cdot\left[\boldsymbol{V}_g^{\pm} + (\boldsymbol{V}-\boldsymbol{V}_g^{\pm})\exp(\mp\sqrt{\mathrm{i}}\eta/\delta)\right] \right.$$
$$\left. -\nabla\cdot\boldsymbol{V}_g^{\pm}\eta \pm \frac{\delta}{\sqrt{\mathrm{i}}}\left[\exp(\mp\sqrt{\mathrm{i}}\eta/\delta)-1\right]\nabla\cdot(\boldsymbol{V}-\boldsymbol{V}_g^{\pm})\right\}\mathrm{e}^{\mathrm{i}\omega t} + \mathrm{cc},$$

where $\eta = z-(f\pm e/2)$, as above, and use has been made of expression (3.5) for the horizontal oscillatory velocity.

Using this result, the variation of the tangential stress across each Stokes layer can be computed by writing the gas momentum equation in the variables $\boldsymbol{x}$ and η, collecting non-oscillatory terms, and integrating the resulting expressions across the layers. The result is, after some algebra,

$$\Delta\boldsymbol{\tau}_{gs}^{\pm} \equiv \rho_g \nu_g \left[\left(\frac{\partial\tilde{\boldsymbol{v}}_{gs}}{\partial\eta}\right)_{\eta=0^{\pm}} - \left(\frac{\partial\tilde{\boldsymbol{v}}_{gs}}{\partial\eta}\right)_{\eta=\pm\infty}\right]$$
$$= \pm\frac{\rho_g\delta}{\sqrt{2}}[\bar{\boldsymbol{V}}_g^{\pm}\cdot\nabla(\bar{\boldsymbol{V}}_g^{\pm}+\mathrm{i}\boldsymbol{V}) - \bar{\boldsymbol{V}}\cdot\nabla(\mathrm{i}\boldsymbol{V}_g^{\pm}+\boldsymbol{V}) + (\bar{\boldsymbol{V}}_g^{\pm}-\bar{\boldsymbol{V}})\nabla\cdot(\mathrm{i}\boldsymbol{V}_g^{\pm}+\boldsymbol{V}) + \mathrm{cc},]$$

where $\tilde{\boldsymbol{v}}_{gs} = \tilde{\boldsymbol{v}}_{gs}(\boldsymbol{x},\eta,t)$ is the horizontal non-oscillatory velocity in the Stokes layers.

Outside the Stokes layers, recalling that $\boldsymbol{v}_{gs} = \boldsymbol{v}_{gs}(\boldsymbol{x},z,t)$ is the non-oscillatory air velocity, we have $(\partial\boldsymbol{v}_{gs}/\partial z)_{z=0^{\pm}} = (\partial\tilde{\boldsymbol{v}}_{gs}/\partial\eta)_{\eta=\pm\infty} - \left[(\partial^2\boldsymbol{V}_g/\partial z^2)\bar{F} + \mathrm{cc}\right]_{z=0^{\pm}}$, the latter term of which is of the order of $|\Delta\boldsymbol{\tau}_{gs}|\delta/(l\rho_g\nu_g)$, with $\Delta\boldsymbol{\tau}_{gs} = \Delta\boldsymbol{\tau}_{gs}^{+} - \Delta\boldsymbol{\tau}_{gs}^{-}$. Therefore, the non-oscillatory stress acting on the film is $\boldsymbol{\tau}_{gs} = \boldsymbol{\tau}_{gs0} + \Delta\boldsymbol{\tau}_{gs}$, where

$$\boldsymbol{\tau}_{gs0} = \rho_g\nu_g\left[\left(\frac{\partial\boldsymbol{v}_{gs}}{\partial z}\right)_{z=0^{+}} - \left(\frac{\partial\boldsymbol{v}_{gs}}{\partial z}\right)_{z=0^{-}}\right] \tag{3.9}$$

is the sum of the non-oscillatory viscous stresses at the outer edges of the Stokes

https://doi.org/10.1017/S0022112098002225 Published online by Cambridge University Press

layers. In what follows the decomposition $\boldsymbol{G} \equiv \boldsymbol{\tau}_{gs}/\rho = \boldsymbol{\tau}_{gs0}/\rho + \boldsymbol{G}_1 + \boldsymbol{G}_2 + \boldsymbol{G}_3$, with

$$\left.\begin{aligned}
\boldsymbol{G}_1 &= \frac{\delta}{\sqrt{2}}\frac{\rho_g}{\rho}\left[\mathrm{i}\bar{\boldsymbol{V}}_g^+(\nabla\cdot\boldsymbol{V}_g^+) + \mathrm{i}\boldsymbol{V}_g^-(\nabla\cdot\bar{\boldsymbol{V}}_g^-) + \mathrm{cc} + 2\nabla(|\boldsymbol{V}_g^+|^2 + |\boldsymbol{V}_g^-|^2)\right],\\
\boldsymbol{G}_2 &= \frac{\delta}{\sqrt{2}}\frac{\rho_g}{\rho}\left[\mathrm{i}(\bar{\boldsymbol{V}}_g^+ + \bar{\boldsymbol{V}}_g^-)\cdot\nabla\boldsymbol{V} - \mathrm{i}\bar{\boldsymbol{V}}\cdot\nabla(\boldsymbol{V}_g^+ + \boldsymbol{V}_g^-) + (\boldsymbol{V}_g^+ + \boldsymbol{V}_g^-)(\nabla\cdot\boldsymbol{V})\right.\\
&\qquad \left. - \mathrm{i}\bar{\boldsymbol{V}}\nabla\cdot(\boldsymbol{V}_g^+ + \boldsymbol{V}_g^-) + \mathrm{cc}\right],\\
\boldsymbol{G}_3 &= -\frac{\delta}{\sqrt{2}}\frac{\rho_g}{\rho}\left[\bar{\boldsymbol{V}}\cdot\nabla\boldsymbol{V} + \bar{\boldsymbol{V}}(\nabla\cdot\boldsymbol{V}) + \mathrm{cc}\right]
\end{aligned}\right\} \tag{3.10}$$

will be used. Here we have taken into account that $\boldsymbol{V}_g^{\pm}$ derives from a potential. Notice that the first two terms in the expression for $\boldsymbol{G}_1$ vanish if the oscillatory flow in the bulk has a spatially uniform phase, as we shall assume in what follows for simplicity. Also, $\boldsymbol{G}_2$ identically vanishes in the symmetric case for which $\boldsymbol{V}_g^+ + \boldsymbol{V}_g^- = \boldsymbol{0}$.

A number of non-oscillatory contributions arise from time averaging the nonlinear terms in the momentum equation for the liquid (2.2). Leaving out the contributions of the viscous terms, which are generally small, the leading-order terms are

$$\left.\begin{aligned}
\boldsymbol{L}_1 &\equiv \left\langle -e\frac{\partial^2 f}{\partial t^2}\nabla f\right\rangle = e_s\omega^2 F\nabla\bar{F} + \mathrm{cc},\\
\boldsymbol{L}_2 &\equiv \langle e\boldsymbol{v}\cdot\nabla\boldsymbol{v}\rangle = e_s\boldsymbol{V}\cdot\nabla\bar{\boldsymbol{V}} + \mathrm{cc},\\
\boldsymbol{L}_3 &\equiv \left\langle e\frac{\partial\boldsymbol{v}}{\partial t}\right\rangle = \mathrm{i}\omega E\bar{\boldsymbol{V}} + \mathrm{cc} = -\bar{\boldsymbol{V}}\nabla\cdot(e_s\boldsymbol{V}) + \mathrm{cc},
\end{aligned}\right\} \tag{3.11}$$

where angular brackets denote time averages over an oscillation period. Here $\boldsymbol{L}_1$, due to the projection of the vertical oscillatory acceleration of the liquid on the oscillatory film, is related to the surface tension force invoked by Airiau (1986) to explain the accumulation of liquid in the crests of the waves. The interpretations in terms of surface tension and of liquid acceleration are equivalent if the effect of the air is neglected.

With $\boldsymbol{L} = \boldsymbol{L}_1 + \boldsymbol{L}_2 + \boldsymbol{L}_3$, the equations governing the quasi-steady streaming in the liquid are

$$\frac{\partial e_s}{\partial t} + \nabla\cdot(e_s\boldsymbol{v}_s) = 0, \tag{3.12a}$$

$$e_s\frac{\partial\boldsymbol{v}_s}{\partial t} + e_s\boldsymbol{v}_s\cdot\nabla\boldsymbol{v}_s = -a_s^2\nabla e_s + \frac{1}{\rho}\nabla\cdot\tau_s' + 2\nu\nabla(e_s\nabla\cdot\boldsymbol{v}_s) + \boldsymbol{G} + \boldsymbol{L}. \tag{3.12b}$$

In summary, the non-oscillatory evolution of the deflection and thickness of the film, f_s and e_s, and of the liquid velocity, $\boldsymbol{v}_s$, is given by equations (3.8) and (3.12). Here $\boldsymbol{V}$ should be obtained from (3.7) and $\boldsymbol{V}_g$ and F from (3.1)–(3.4) (plus boundary conditions), while $\boldsymbol{\tau}_{gs0}$ depends on the non-oscillatory air flow outside the Stokes layers, which will be discussed below briefly. In addition, (3.8) and (3.12) must be supplemented with appropriate initial and boundary conditions, which depend on the mode of film attachment to the frame and will not be discussed here.

Consider now the limits of validity of the analysis leading to (3.8) and (3.12). A detailed scrutiny of neglected terms shows that these limits are

$$|\boldsymbol{v}_s| + |\boldsymbol{V}_g| + |\boldsymbol{V}| \ll \omega l, \quad \frac{|\boldsymbol{V}|^2}{\omega l} \ll |\boldsymbol{v}_s|, \quad \left(R + R^{1/2}\right)\frac{|\boldsymbol{V}_g|^2}{\omega l} \ll |\boldsymbol{v}_s|, \tag{3.13}$$

https://doi.org/10.1017/S0022112098002225 Published online by Cambridge University Press

where again $R = (\rho_g \delta)/(\rho e_c)$. The first limit comes from neglecting convective terms in the linear approximations (3.1)–(3.4) and (3.7), as previously noted. Convective terms should be added to these linear problems if $|\boldsymbol{v}_s| = O(\omega l)$ or larger, while the oscillatory motions of the air or the liquid become fully nonlinear if $|\boldsymbol{V}_g| = O(\omega l)$ or $|\boldsymbol{V}| = O(\omega l)$. The other two conditions, establishing lower bounds on $|\boldsymbol{v}_s|$, stem from requiring that the largest neglected terms in the expressions for $\boldsymbol{L}$ and $\boldsymbol{G}$ be small compared to the convective terms in equation (3.12*b*). The first of these conditions is a consequence of neglecting, in $\boldsymbol{L}_2$ and $\boldsymbol{L}_3$, terms of the type $\bar{E}\,(\boldsymbol{v}_s\cdot\nabla\boldsymbol{V}+\boldsymbol{V}\cdot\nabla\boldsymbol{v}_s)+e_s\,(\boldsymbol{V}_1\cdot\nabla\bar{\boldsymbol{V}}+\bar{\boldsymbol{V}}\cdot\nabla\boldsymbol{V}_1)+\text{cc}$, where $\boldsymbol{V}_1$ is the second approximation to the oscillatory flow in the liquid, of order $|\boldsymbol{V}||\boldsymbol{v}_s|/(\omega l)$. The second lower bound on $|\boldsymbol{v}_s|$ is the result of neglecting similar terms in the Stokes layers.

The non-oscillatory three-dimensional flow of the air outside the Stokes layers should be computed in order to determine $\boldsymbol{\tau}_{gs0}$. We now estimate the order of this term and the condition under which its effect can be neglected in (3.12). The non-oscillatory air flow is driven by the quasi-steady velocities extant at the outer edges of the Stokes layers on the solid walls and on the film. These velocities are of orders $|\boldsymbol{V}_g|^2/(\omega l)$ and $|\boldsymbol{v}_s| + |\boldsymbol{V}_g|^2/(\omega l)$, respectively, and typically lead to a high Reynolds number gas flow with non-oscillatory boundary layers on the walls and on the film. The latter have a thickness of order $[|\boldsymbol{v}_s| + |\boldsymbol{V}_g|^2/(\omega l)]^{-1/2}(\nu_g l)^{1/2}$, and therefore $\boldsymbol{\tau}_{gs0} = O\{\rho_g \nu_g^{1/2}[|\boldsymbol{v}_s| + |\boldsymbol{V}_g|^2/(\omega l)]^{3/2}/l^{1/2}\}$. This term can be neglected relative to the convective terms in (3.12) when

$$R^2\omega l + R^{1/2}\frac{|\boldsymbol{V}_g|^{3/2}}{(\omega l)^{1/2}} \ll |\boldsymbol{v}_s|. \tag{3.14}$$

This condition is compatible with (3.13) only if the parameter R is small. The effect of $\boldsymbol{\tau}_{gs0}$ cannot be neglected when R is of order unity, which happens for sufficiently thin films, of the order of 0.1 μm. Experimentally it is observed that thin films display interesting features which could well be explained by this effect. However, $\boldsymbol{\tau}_{gs0}$ depends on the presence and location of the walls, and thus such features are somewhat peripheral to the main theme of our work. Consequently, we shall focus on the case when (3.14) is satisfied and the effect of the outer non-oscillatory gas flow can be neglected.

3.3. *Orders of magnitude and discussion*

Granted that (3.13) and (3.14) are satisfied, the following remarks can be made. First, inspection of (3.10) and (3.11) immediately shows that $\boldsymbol{G}_1 = O(e_c R|\boldsymbol{V}_g|^2/l)$, $\boldsymbol{G}_2 = O(e_c R|\boldsymbol{V}_g||\boldsymbol{V}|/l)$, $\boldsymbol{G}_3 = O(e_c R|\boldsymbol{V}|^2/l)$, and $\boldsymbol{L}_1 = O(e_c|\boldsymbol{V}_g|^2/l)$, $(\boldsymbol{L}_2, \boldsymbol{L}_3) = O(e_c|\boldsymbol{V}|^2/l)$. Here use has been made of the relation $\omega|F| = O(|\boldsymbol{V}_g|)$ in the estimate of $\boldsymbol{L}_1$ and e_c is the characteristic value of the film thickness, as mentioned before, while $a_c = a(e_c)$ will be used below as the characteristic speed of the Marangoni waves. Since R is small, $\boldsymbol{G}_1$ is smaller than $\boldsymbol{L}_1$, and $\boldsymbol{G}_3$ is smaller than $\boldsymbol{L}_2$ and $\boldsymbol{L}_3$. Second, both $\boldsymbol{G}_1$ and $\boldsymbol{L}_1/e_s$ are gradients of scalar functions if the oscillatory gas flow has a spatially uniform phase, as we are assuming here. Third, some asymmetry is necessary to excite Marangoni waves in the liquid, because $f_s = 0$ and $\boldsymbol{V} = \boldsymbol{0}$ in the purely symmetric case when $\boldsymbol{V}_g^+ + \boldsymbol{V}_g^- = \boldsymbol{0}$ and gravity is neglected (cf. (3.7) and (3.8)).

Two cases arise depending on the amplitude of the oscillations of the gas:

(*A*) Assume first that $|\boldsymbol{V}_g| \ll a_c$, which in the realistic case $\omega l = O(a_c)$ amounts to $|\boldsymbol{V}_g| \ll \omega l$, as required in (3.13). The balance of the largest forcing terms, of order $e_c(|\boldsymbol{V}_g|^2 + |\boldsymbol{V}|^2)/l$, with the Marangoni force $-a_s^2\nabla e_s$ in (3.12) yields $\Delta e_s/e_s = O\left[\left(|\boldsymbol{V}_g|^2 + |\boldsymbol{V}|^2\right)/a_c^2\right]$, where Δe_s is the non-oscillatory thickness variation due to

https://doi.org/10.1017/S0022112098002225 Published online by Cambridge University Press

the motion of the liquid. The order of magnitude of $\boldsymbol{V}$, which was obtained in the paragraph following equation (3.7), depends on whether a Marangoni mode resonates and on the order of $|\nabla f_s| + g/(\omega^2 l)$, but in most cases $V \ll a_c$, and therefore, $\Delta e_s/e_s \ll 1$. This implies that, in the absence of mechanisms to vary the film thickness other than the non-oscillatory motion of the liquid, e_s can be replaced by a constant everywhere in (3.12) except in ∇e_s appearing in the Marangoni term, and these equations then reduce to those describing the two-dimensional motion of an incompressible fluid.

Experiments (Airiau 1986; Afenchenko *et al.* 1998), however, show that large spatial variations of thickness often exist in vibrating films displaying vortical motion. These variations may be initially present or may be generated by differential soap–water evaporation in the presence of air streaming, or by other causes (see also case *B* below). Insofar as the thickness variations are not due directly to the non-oscillatory motion of the liquid, the time derivative in equation (3.12*a*) can be neglected, which amounts to eliminating acoustics from the non-oscillatory flow. A possible additional complication brought about by the mechanism leading to thickness non-uniformities is that it may also change the surfactant concentration in such a way that σ_s and a_s are not only functions of e_s but depend explicitly on $\boldsymbol{x}$, a possibility not accounted for in the present formulation.

The order of magnitude of $|\boldsymbol{v}_s|$ depends on whether a Marangoni mode resonates or not. The two cases are now discussed in turn.

(*A*.1) If ω is close to a Marangoni eigenfrequency then $|\boldsymbol{V}|$ is of the order of $|\boldsymbol{V}_g|$, or even larger than $|\boldsymbol{V}_g|$ if $|\nabla f_s| + g/(\omega^2 l) \gg R$, which may happen for thick films. In this case $\boldsymbol{V}$ is a Marangoni eigenfunction in the first approximation, which can be written as $\boldsymbol{V} = e_s^{-1}\nabla\Phi$ for some potential Φ. Since R is small, the largest forcing terms, of order $e_c(|\boldsymbol{V}|^2 + |\boldsymbol{V}_g|^2)/l$, come from $\boldsymbol{L}$ which can be written as

$$\boldsymbol{L} = e_s\left[\omega^2\nabla(|F|^2) + e_s^{-2}\nabla(|\nabla\Phi|^2) - \left(e_s^{-2}(\nabla^2\Phi)\nabla\bar{\Phi} + \mathrm{cc}\right)\right] - 2|\Phi_x + \Phi_y|^2 e_s^{-2}\nabla e_s. \quad (3.15)$$

This forcing would derive from a potential if e_s were strictly uniform. Then it could be absorbed into the Marangoni term and would not lead to any motion of the liquid. The flow in this case, therefore, is closely associated with thickness non-uniformities. If the only non-uniformities are due to the non-oscillatory motion of the liquid, substitution of (3.15) into (3.12*b*) yields $|\boldsymbol{v}_s| = 0\left\{(|\boldsymbol{V}|^2 + |\boldsymbol{V}_g|^2)/a_c\right\}$. If $\Delta e_s/e_s = O(1)$, on the other hand, much larger velocities, of order $|\boldsymbol{V}| + |\boldsymbol{V}_g|$, are generated. This difference may explain the noticeable motion observed by Afenchenko *et al.* (1998) around regions of black film, where e_s is small and rapidly increasing away from such regions.

(*A*.2) If no Marangoni mode resonates then the estimate of $|\boldsymbol{V}|$ in the paragraph following equation (3.7) implies that $|\boldsymbol{V}| \ll |\boldsymbol{V}_g|$, provided that $g \ll \omega^2 l$, as is the case in most experiments. For these conditions $|\boldsymbol{L}_1| \gg (|\boldsymbol{L}_2|, |\boldsymbol{L}_3|)$ and $|\boldsymbol{G}_1| \gg |\boldsymbol{G}_2| \gg |\boldsymbol{G}_3|$. The largest forcing term in (3.12*b*) is $\boldsymbol{L}_1$, but it can be absorbed into the Marangoni term and does not lead to any motion of the liquid. The next largest forcing terms not given by the gradient of a potential are $\boldsymbol{G}_2$ and $\boldsymbol{L}_3$, and their sum generates a non-oscillatory motion in the film with velocity $|\boldsymbol{v}_s| = O\left\{|\boldsymbol{V}| + (R|\boldsymbol{V}||\boldsymbol{V}_g|)^{1/2}\right\}$, where $|\boldsymbol{V}| = 0\left\{R|\boldsymbol{V}_g^+ + \boldsymbol{V}_g^-| + [|\nabla f_s| + g/(\omega^2 l)]|\boldsymbol{V}_g|\right\}$, with f_s as given by equation (3.8). Notice that this motion does not rely on thickness non-uniformities, and that it is fairly weak, such that $|\boldsymbol{v}_s| \ll |\boldsymbol{V}_g| \ll a_c$. (Recall that the present analysis breaks down if the consistency requirements (3.13) and (3.14) are violated.)

The reason neither $\boldsymbol{G}_2$ nor $\boldsymbol{L}_3$ can be derived from a potential may be worth

https://doi.org/10.1017/S0022112098002225 Published online by Cambridge University Press

mentioning here. Equation (3.7) shows that even if $\boldsymbol{V} = \nabla\Phi$ for some potential Φ, which would be the case if the second term on the right-hand side of this equation were neglected and e_s and a_s are constant, that potential is not proportional to its own Laplacian because neither F nor the potential of $\boldsymbol{V}_g^+ + \boldsymbol{V}_g^-$ (when $\boldsymbol{V}_g^+ + \boldsymbol{V}_g^- \neq \boldsymbol{0}$) satisfy this condition for a film of finite size. As can be verified using (3.10) and (3.11), this prevents $\boldsymbol{G}_2$ and $\boldsymbol{L}_3$ from being potential.

(B) Assume now that $|\boldsymbol{V}_g| \not\ll a_c$, which in the framework of the present weakly nonlinear analysis can happen only if ωl is somewhat larger than a, rendering Marangoni modes difficult to excite. The forcing $\boldsymbol{L}_1$ leads to $\Delta e_s/e_s = O(1)$ but does not generate any motion by itself. The terms $\boldsymbol{L}_2$ and $\boldsymbol{L}_3$ would be much larger than $\boldsymbol{G}$ if a Marangoni mode could still resonate, leading to $|\boldsymbol{v}_s| = O(a_c)$, a condition apparently never observed experimentally. If there are no resonances, then $\boldsymbol{L}_2$ and $\boldsymbol{L}_3$ are likely to be smaller than the potential part of $\boldsymbol{G}$, so at leading order the forcing in (3.12) is of the form $e_s\nabla\Phi_{_L} + \nabla\Phi_{_G}$, where $\Phi_{_L} = \omega^2|F|^2 = O(|\boldsymbol{V}_g|^2)$ (from $\boldsymbol{L}_1$) and $\Phi_{_G} = (\sqrt{2}\delta\rho_g/\rho)(|\boldsymbol{V}_g^+|^2 + |\boldsymbol{V}_g^-|^2) = O(e_c R|\boldsymbol{V}_g|^2) \ll e_s\Phi_{_L}$ (from $\boldsymbol{G}_1$). This combination of volume and surface potential forcing cannot be absorbed by a Marangoni force alone if $\Phi_{_L}$ and $\Phi_{_G}$ are not functions of each other, and leads to $|\boldsymbol{v}_s| = O(R^{1/2}|\boldsymbol{V}_g|)$.

The mechanism of volume plus surface potential forcing also exists for small values of $|\boldsymbol{V}_g|/a_c$. Then each of the forcing terms can be separately absorbed into small changes of thickness Δe_s, but these changes lead to the small term $\Delta e_s\nabla\Phi_{_L}$, which, though formally of higher order in expansions (2.4) and (2.5), can still induce an observable motion in the liquid, along with other higher-order terms not included in (3.11).

4. Numerical solutions

Numerical solutions of (3.12) are now presented and discussed. These computations are not intended to reproduce the results of any specific experiment, but to generate insight into the type of flows allowed by (3.12) with typical forcing terms. Such an approach permits a number of simplifications. First, equations (3.12) are solved with periodic boundary conditions, which at best amounts to describing the flow in a limited region of the film away from the frame. This is possible, in principle, because the forcing described in the previous section acts on the whole film, so that the quasi-steady streaming need not be dominated by boundary effects. Moreover, any other boundary condition, reckoning the finite extent of the film, would require an analysis of the flow in the vicinity of the frame, which is both complicated and problem dependent. Second, simplified forms of $\boldsymbol{G}$ and $\boldsymbol{L}$ will be used instead of the full expressions (3.10) and (3.11). Again, evaluation of (3.10) and (3.11) would require knowledge of the oscillatory fields, which depend on the geometrical configuration of the frame and the cavity and on details of the mechanism used to excite the vibrations. We have already pointed out that some important features of the forcing depend on properties of the oscillatory fields related to the finite extent of the film, but these features can be easily taken into account in the simplified forms of $\boldsymbol{G}$ and $\boldsymbol{L}$.

Equations (3.12) are rewritten in non-dimensional form by scaling $(\boldsymbol{x}, t, e_s, \boldsymbol{v}_s)$ with $(l, l/v_c, e_c, v_c)$, where l is the spatial period of the flow, the same in both horizontal directions, e_c is a characteristic thickness, and $v_c = \left[2c/\rho(e_c + k)\right]^{1/2}$. In these variables, $a_s^2 = K(1{+}K)/(e{+}K)$, with $K = k/e_c$, and the non-dimensional parameters $Re = v_c l/\nu$ and $N = \nu^s/e_c\nu$ appear. Parameter values $K = N = 1$ and $Re = 500$ are chosen unless otherwise noted. The non-dimensional equations are discretized using a second-order

https://doi.org/10.1017/S0022112098002225 Published online by Cambridge University Press

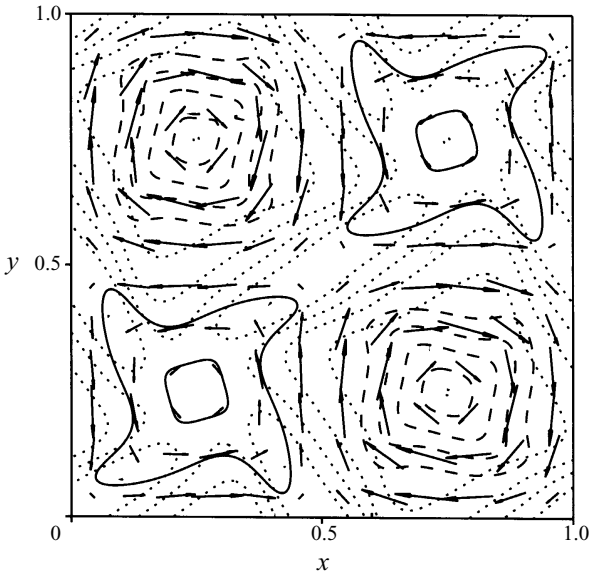


FIGURE 1. Solution of (3.12) with $\boldsymbol{L} = e_s \nabla \Phi_L$ and $\boldsymbol{G} = 0.2\,(\partial \Phi_L/\partial y, -\partial \Phi_L/\partial x)$, where $\Phi_L = 0.5 \sin(2\pi x) \sin(2\pi y)$. Plotted are six equispaced contours of e_s between 0.15 and 2.02 (dotted), six contours of the vorticity (ω_s) between -20 and 10 (solid for $\omega_s > 0$ and dashed for $\omega_s < 0$), and velocity arrows.

finite difference scheme with artificial viscosity, and marched in time with a fourth-order Runge–Kutta method; see Hirsch (1990).

A number of computations have been carried out with different forcing terms (non-dimensionalized with $e_c v_c^2/l$). The large potential forcing $\boldsymbol{L}_1 = e_s \nabla \Phi_L$ was represented using $\Phi_L = A \sin(2\pi m x) \sin(2\pi n y)$, with $A = 0.5$ and $m = n = 1$ in most of the cases. As was discussed in § 3.3, this forcing does not induce any motion by itself, but leads to a spatial thickness variation that enables or enhances the action of other terms. Moreover, it is assumed that the potential forcing may also approximately simulate thickness variations whose real origin is a variation of surface tension not due to any quasi-steady forcing, a feature not included in our formulation. Thus, in order to mimic the strong recirculations sometimes observed in variable thickness regions around patches of black film (which, strictly, are outside the framework of the present model), a non-potential forcing $\boldsymbol{G} = (\partial \Phi_G/\partial y, -\partial \Phi_G/\partial x)$, with $\Phi_G = 0.2\,\Phi_L$, was added to $\boldsymbol{L}_1$. $\boldsymbol{G}$ is taken orthogonal to $\boldsymbol{L}_1$ because an additional $\boldsymbol{G}$ with a component parallel to the larger forcing $\boldsymbol{L}_1$ generates only a weak perturbation to the motion, one partially masked by $\boldsymbol{L}_1$. Contours of constant thickness (dotted) and of vorticity (solid for $\omega_s > 0$ and dashed for $\omega_s < 0$), along with some velocity arrows, are displayed in figure 1. The thickness is maximum in the ridge at the centre of the figure and in four other ridges on the sides. These ridges connect passages of relatively large thickness (in the first and third quadrants of the figure) and leave valleys of small thickness (in the second and fourth quadrants). As can be seen, the clockwise circulation around the two valleys is stronger than the counterclockwise circulation around the two passages. Increasing f produces a time-periodic flow, with a thickness maximum moving back and forth along each ridge. In the figure, four maxima would converge alternatively onto the passages in the first and third quadrants and the circulations would pulsate in counterphase.

https://doi.org/10.1017/S0022112098002225 Published online by Cambridge University Press

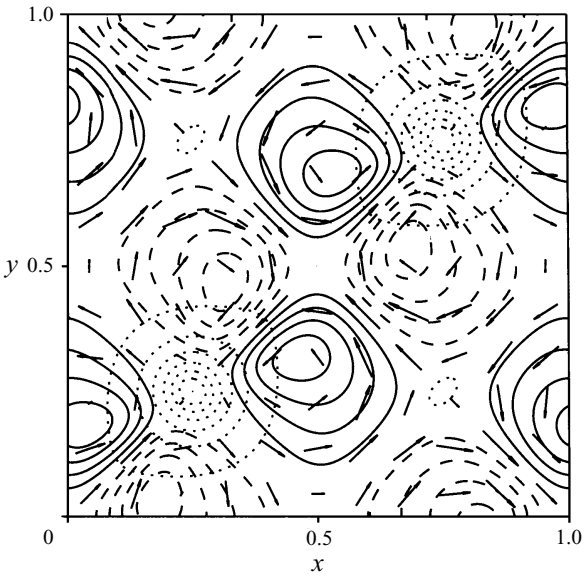


FIGURE 2. Solution of (3.12) with $\boldsymbol{L} = e_s \nabla \Phi_L$ and $\boldsymbol{G} = \nabla \Phi_G$, where $\Phi_L = 0.5 \sin(2\pi x) \sin(2\pi y)$ and $\Phi_G = 0.1 \sin(2\pi x + \pi/2) \sin(2\pi y + \pi/2)$. Plotted are eight equispaced contours of e_s between 0.44 and 5.83 (dotted), eight contours of the vorticity between -4 and 4 (solid for $\omega_s > 0$ and dashed for $\omega_s < 0$), and velocity arrows.

The mechanism of volume plus surface forcing is illustrated in figure 2 for the same Φ_L of the previous case and $\Phi_G = B \sin(2\pi x + \pi/2) \sin(2\pi y + \pi/2)$, with $B = 0.1$. As can be seen, four vortices of alternate signs appear around each of the two 'bladders' of large thickness on the main diagonal; two vortices with positive circulation at the left and right and two with negative circulations above and below. Again the velocity is higher outside the bladders than inside. The centres of the vortices are not far from the extremes of the vorticity source term $\nabla e_s^{-1} \times \nabla \Phi_G$, with e_s roughly proportional to Φ_L. Replacing Φ_G with Φ_G^2 the flow develops eight vortices around each bladder.

These configurations, in particular the one with four vortices per bladder which was studied more intensively, proved fairly robust. No stability analysis has been carried out, but all the velocity and thickness perturbations that were tried, including both harmonics and sub-harmonics of the forcing, were observed to decay in time when the values of A and B of the previous simulation were used. The stationary structure becomes less stable when A is decreased. Decreasing A reduces the thickness variation due to the potential forcing $\boldsymbol{L}_1$ and the strength of the vorticity source, but at the same time renders the thickness variation due to the motion comparatively more important, so the flow ceases to be pinned to specific locations on the film. A non-stationary flow was setup by adding sub-harmonic perturbations, of wavelength equal to two non-dimensional units, to the stationary flow with $A = 0.2$ and $Re = 2000$. The increase of Re is required to keep viscous effects small, because the non-dimensional velocity decreases rapidly with decreasing values of A. In the transient solution the peaks of maximum thickness oscillate smoothly along the main diagonal of figure 2 whilst the surrounding vortices suffer very large deformations. Moreover, the Marangoni waves do not disappear with the present periodic boundary conditions, but instead lead to fast oscillations that coexist with the slower evolution of the vorticity in the film.

As was mentioned in § 3.3 (case A), the governing equations reduce to a description

https://doi.org/10.1017/S0022112098002225 Published online by Cambridge University Press

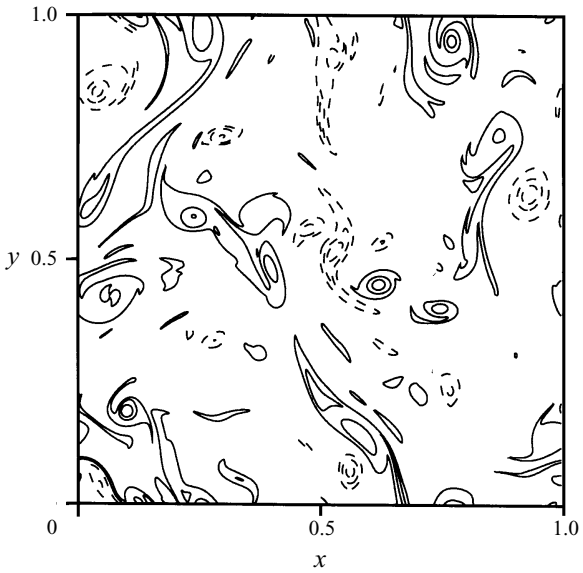


FIGURE 3. Eight equispaced vorticity contours between −3 and +3 from the numerical solution of (4.1) with 768^2 Fourier modes. A thin shell of modes around $|\boldsymbol{k}| = 10$ are forced with amplitude 0.05, and $Re/(1+N) = 5000$ based on the r.m.s. velocity.

of two-dimensional incompressible flow when the velocities involved are much smaller than the speed of Marangoni waves and only the small thickness variations due to the motion of the liquid are present. In this case (3.12) can be rewritten in the vorticity–stream function form

$$\left.\begin{aligned} &\nabla^2\psi_s = -\omega_s, \quad \text{with} \quad (u_s, v_s) = \left(\frac{\partial\psi_s}{\partial y}, -\frac{\partial\psi_s}{\partial x}\right), \\ &\frac{\partial\omega_s}{\partial t} + \boldsymbol{v}_s \cdot \nabla\omega_s = \frac{1+N}{Re}\nabla^2\omega_s + \Omega, \end{aligned}\right\} \tag{4.1}$$

where $\omega_s = (\nabla \times \boldsymbol{v}_s)_z = (\partial v_s/\partial x - \partial u_s/\partial y)$ is the vorticity and $\Omega = [\nabla \times (\boldsymbol{G} + \boldsymbol{L})]_z$. Here the velocity has been non-dimensionalized with $\Omega_c^{1/2} l$, where Ω_c is a characteristic value of the vorticity forcing term. Equations (4.1) were solved with a spectral method. The stationary solution for $\Omega = \sin(2\pi x)\sin(2\pi y)$ and $Re/(1+N) = 500$, consisting of a lattice of counter-rotating vortices not very different from the ones of figure 2, is unstable to sub-harmonic disturbances, which induce vortex pairings in a well-known fashion (see, e.g., Batchelor 1969 and McWilliams 1990). The vorticity distribution for $Re/(1+N) = 5000$ (based on the resulting r.m.s. velocity) is shown in figure 3 after about ten large eddy turn-over times, when several pairings have already occurred. This computation was carried out with 768^2 Fourier modes, a shell of modes around $|\boldsymbol{k}| = 10$ being isotropically forced with amplitude 0.05. The results resemble some of the visualizations of Afenchenko *et al.* (1998) of thin large square films.

5. Conclusions

An analysis has been carried out of the quasi-steady streaming in a vibrated horizontal soap film. The salient features of the oscillatory and quasi-steady flows are recapitulated below.

https://doi.org/10.1017/S0022112098002225 Published online by Cambridge University Press

The air surrounding the film is often the vehicle transmitting the vibration from the excitation source, and the inertia of this air is almost always important to the dynamics of the oscillations. Stokes layers existing in the air on both sides of the soap film transmit an oscillatory shear stress which causes oscillations of the liquid tangent to the film in all but special cases characterized by a symmetry that prevents the existence of such oscillatory stress. The amplitude of the tangential oscillation of the liquid may be large if a Marangoni mode is excited by this means.

In general, the oscillatory velocity of the air at the outer edges of the Stokes layers on the soap film will be neither parallel nor perpendicular to the film, but at an angle that depends on the local position on the film. The component of this velocity normal to the unperturbed film is continuous across the Stokes layers in first approximation, and is equal to the velocity of the oscillatory deflection of the film. In turn, this velocity is much larger than the velocity of the liquid tangent to the film, except when a Marangoni mode resonates. Marangoni waves may of course be excited by an oscillatory motion of the air everywhere tangent to the film, a type of excitation that would not lead to flexural oscillations. This particular forcing would require a specifically designed acoustic device. The analysis of § 3.3 applies to this type of motion with the only modification that the deflection of the film, being zero, can no longer be used as a measure of the amplitude of the air oscillation, and should be replaced by A_0 appearing in the paragraph following (3.5). Yet another possibility is to excite Marangoni waves without recourse to the air, by vibrating the film support frame tangentially to the film. The efficiency of this method, however, should be expected to depend on the conditions of attachment of the film to its frame, and will not be discussed here.

Due to the nonlinearity of the problem, the oscillation of the air generates a non-oscillatory pressure variation that leads to a non-oscillatory normal force on the film. This force, along with the weight of the liquid and another normal force generated by nonlinear effects inside the liquid, are balanced by surface tension in a manner that produces a non-oscillatory, quasi-steady deflection of the film.

A non-oscillatory motion of the liquid tangent to the film is induced by non-oscillatory volume forcing due to nonlinear effects inside the liquid, and by non-oscillatory surface shear stresses due to nonlinear effects in the Stokes layers in the air. In addition, these layers and the ones on the solid walls confining the film in a closed cavity induce a non-oscillatory flow in the air which exerts an extra shear stress on the film. Explicit expressions for the forcing terms due to the liquid and the Stokes layers in the air, in terms of the oscillatory velocities in both phases and the oscillatory deflection of the film, are worked out. The stress due to the streaming of the air, which depends on the geometrical configuration of the film and the surrounding walls, is estimated.

Bulk forcing is larger than surface forcing when the excitation frequency is close to the eigenfrequency of a Marangoni mode of the film. Then the former forcing leads to a non-oscillatory liquid flow only in the presence of variations of the film thickness, which may be due to the motion of the liquid or to other causes. If no Marangoni mode resonates, a weaker motion is induced in the liquid both by volume and surface forcing, which are not crucially dependent on the non-uniformity of film thickness. Several possible ways in which the combined action of the different forcings may induce vortex motion are identified, and three numerical simulations of the flow in the liquid film are presented which rely on simplified forms of the forcing terms.

Owing to the complex rheology of soap films, it is likely that variations of thickness exist in the soap film due to causes not accounted for in the present formulation, and

https://doi.org/10.1017/S0022112098002225 Published online by Cambridge University Press

in some cases such variations bear on the efficiency of the forcing to generate motion in the liquid. In some of the simulations presented here, the necessary thickness variations have been obtained by means of an exaggerated potential forcing.

The effect of an inclination of the film support frame to the horizontal is of interest. After an initial transient, an inclined film reaches a nearly stationary state with a thickness that decreases with upward distance (Couder *et al.* 1989). Subsequently the film thins down due to marginal regeneration (Mysels, Shinoda & Frankel 1959), but this process is probably too slow to matter much here. The influence of the component of gravity tangent to the film on the flexural and Marangoni oscillations comes through its contribution to the coefficients e_s and σ_s in (3.4) and (3.7). These coefficients are determined by equations (3.12), which should be augmented by adding a new term to $\boldsymbol{L}$, equal to e_s times the projection of the gravitational acceleration on the surface of the film. Equations (3.12) with this new forcing term alone would give the evolution of the film toward the nearly stationary state mentioned above. The characteristic time of this evolution may be similar to the characteristic time of the quasi-steady streaming which equations (3.12) are intended to describe so that, depending on the experimental set up, both processes could occur simultaneously. Moreover, the relative thickness variation due to gravity in a sufficiently large inclined film may be $\Delta e_s/e_s = O(1)$, in which case the ability of the other forcing terms to generate vortical motions would be very much enhanced, as discussed in § 3.3.

We gratefully acknowledge the help of A. Pinelli and C. Vasco with the numerical solution of (4.1). This work was partially supported by DGICYT grants PB95-0008 and PB97-0556, and by NASA grant NAG3-2152.

REFERENCES

Afenchenko, V. O., Ezersky, A. B., Kiyashko, S. V., Rabinovich, M. I. & Weidman, P. D. 1998 The generation of two-dimensional vortices by transverse oscillation of a soap film. *Phys. Fluids* **10**, 390–399.

Airiau, M. 1986 Etude des vibrations des membranes de savon. *DEA Rep.*, Ecole Normale Supérieure, Paris.

Batchelor, G. K. 1969 Computation of the energy spectrum in homogeneous two-dimensional turbulence. *Phys. Fluids* **12**, II-233–II-239.

Bergmann, L. 1956 Experiments with vibrating soap membranes. *J. Acoust. Soc. Am.* **28**, 1043–1047.

Chomaz, J. M., Rabaud, M., Basdevant, C. & Couder, Y. 1988 Experimental and numerical investigation of a forced circular shear layer. *J. Fluid Mech.* **187**, 115–140.

Couder, Y. 1981 The observation of a shear flow instability in a rotating system with a soap membrane. *J. Phys. Lett.* **42**, 429–431.

Couder, Y. 1984 Two-dimensional grid turbulence in a thin liquid film. *J. Phys. Lett.* **45**, 353–360.

Couder, Y. & Basdevant, C. 1986 Experimental and numerical study of vortex couples in two-dimensional flows *J. Fluid Mech.* **173**, 225–251.

Couder, Y., Chomaz, J. M. & Rabaud, M. 1989 On the hydrodynamics of soap films. *Physica* D **37**, 384–405.

Dewar, J. 1923 Soap films as detectors: Streamlines and sound. *Proc. Roy. Inst.* **24**, 197–259. (See also *Collected Papers of Sir James Dewar*, vol. 2, pp. 1334–1379. Cambridge University Press 1927.)

Gharib, M. & Derango, P. 1989 A liquid film (soap film) tunnel to study two-dimensional laminar and turbulent shear flows. *Physica* D **37**, 406–416.

Gibbs, J. W. 1931 *The Collected Works.* Longmans Green.

Hirsch, C. 1990 *Numerical Computation of Internal and External Flows,* vol. 2, chaps. 18 and 23. Wiley.

https://doi.org/10.1017/S0022112098002225 Published online by Cambridge University Press

Jenkins, A. D. & Dysthe, K. B. 1997 The effective film viscosity of a thin floating fluid layer. *J. Fluid Mech.* **344**, 335–337.

Martin, B. K., Wu, X. L. & Goldburg, W. I. 1998 Spectra of decaying turbulence in a soap film. *Phys. Rev. Lett*. **80**, 3964–3967.

McWilliams, J. C. 1990 The vortices of two-dimensional turbulence. *J. Fluid Mech.* **219**, 361–385.

Mysels, K. J., Shinoda, K. & Frankel, S. 1959 *Soap Films, Studies of Their Thinning*. Pergamon.

Plateau, J. 1873 *Statique Expérimentale et Thèorique des Liquides Soumis aux Seules Forces Moléculaires*. Gauthier-Villars.

Rabaud, M. & Couder, Y. 1983 A shear-flow instability in a circular geometry. *J. Fluid Mech.* **136**, 291–319.

Riley, N. 1997 Acoustic streaming. In *Encyclopedia of Acoustics* (ed. M. J. Crocker). Wiley.

Rusanov, A. I. & Krotov, V. V. 1979 Gibbs elasticity of liquid films, threads and foams. *Progr. Surf. Membrane Sci.* **13**, 415–524.

Rutgers, M. A., Wu, X.-I. & Bhagavatula, R. 1996 Two-dimensional velocity profiles and laminar boundary layers in flowing soap films. *Phys. Fluids* **8**, 2847–2854.

Schlichting, H. 1951 *Boundary layer theory*. McGraw Hill.

Taylor, G. I. 1959 The dynamics of thin sheets of fluid II. Waves on fluid sheets. *Proc. R. Soc. Lond.* A **253**, 296–312.

Taylor, S. 1878 Colours shown by thin liquid films under the action of sonorous vibrations *Proc. R. Soc. Lond.* **27**, 71–76.

https://doi.org/10.1017/S0022112098002225 Published online by Cambridge University Press